Steel and Composite Structures, Vol. 14, No. 1 (2013) 85-104
DOI: http://dx.doi.org/10.12989/scs.2013.14.1.085

Thermomechanical bending response of FGM thick plates resting on Winkler-Pasternak elastic foundations

Bachir Bouderba[1], Mohammed Sid Ahmed Houari[1,2] and Abdelouahed Tounsi[*1,3]

[1] *Laboratoire des Matériaux et Hydrologie, Université de Sidi Bel Abbes, BP 89 Cité Ben M'hidi 22000 Sidi Bel Abbes, Algérie*
[2] *Département de Génie Civil, Faculté des Sciences et Technologie, Université de Mascara, Algérie*
[3] *Département de Génie Civil, Faculté de Technologie, Université Sidi Bel Abbes, Algérie*

(Received June 11, 2012, Revised November 25, 2012, Accepted November 30, 2012)

Abstract. The present work deals with the thermomechanical bending response of functionally graded plates resting on Winkler-Pasternak elastic foundations. Theoretical formulations are based on a recently developed refined trigonometric shear deformation theory (RTSDT). The theory accounts for trigonometric distribution of transverse shear stress, and satisfies the free transverse shear stress conditions on the top and bottom surfaces of the plate without using shear correction factor. Unlike the conventional trigonometric shear deformation theory, the present refined trigonometric shear deformation theory contains only four unknowns as against five in case of other shear deformation theories. The material properties of the functionally graded plates are assumed to vary continuously through the thickness, according to a simple power law distribution of the volume fraction of the constituents. The elastic foundation is modelled as two-parameter Pasternak foundation. The results of the shear deformation theories are compared together. Numerical examples cover the effects of the gradient index, plate aspect ratio, side-to-thickness ratio and elastic foundation parameters on the thermomechanical behavior of functionally graded plates. It can be concluded that the proposed theory is accurate and efficient in predicting the thermomechanical bending response of functionally graded plates.

Keywords: refined plate theory; thermomechanical loading; FGM; elastic foundations

1. Introduction

The increased applications of advanced composite materials in structural members have stimulated interest in the accurate prediction of the response characteristics of functionally graded (FG) plates used in situations where large temperature gradients are encountered. Functionally graded materials (FGMs) are designed so that material properties vary smoothly and continuously through the thickness from the surface of a ceramic exposed to high temperature to that of a metal on the other surface. The mechanical properties are graded in the thickness direction according to volume fraction power law distribution. Since the main applications of FGMs have been in high temperature environments, most of the research on FGMs has been restricted to thermomechanical stress analysis, thermal buckling, fracture mechanics and optimization.

*Corresponding author, Professor, E-mail: tou_abdel@yahoo.com

Plates supported by elastic foundations have been widely adopted by many researchers to model various engineering problems during the past decades. To describe the interactions of the plate and foundation as more appropriate as possible, scientists have proposed various kinds of foundation models, as documented well in Ref. (Kerr 1964). The simplest model for the elastic foundation is the Winkler model, which regards the foundation as a series of separated springs without coupling effects between each other, resulting in the disadvantage of discontinuous deflection on the interacted surface of the plate. This was later improved by Pasternak (1954) who took account of the interactions between the separated springs in the Winkler model by introducing a new dependent parameter. From then on, the Pasternak model was widely used to describe the mechanical behavior of structure–foundation interactions (Omurtag *et al*. 1997, Matsunaga 2000, Filipich and Rosales 2002, Zhou *et al.* 2004, Behravan Rad 2012).

The thermomechanical bending response of thick plates made of FGMs is of great interest for engineering design and manufacture. Reddy (2000) and Reddy and Cheng (2001) have used an asymptotic method to determine three-dimensional thermomechanical deformations of FG rectangular plates. Cheng and Batra (2000) have used the method of asymptotic expansion to study the 3D thermoelastic deformations of an FG elliptic plate. Vel and Batra (2002) have presented an exact 3D solution for the thermoelastic deformation of FG simply supported plates of finite dimensions. Ying *et al*. (2009) used a semi-analytical method to study thermal deformations of FG thick plates and the analysis is directly based on the 3D theory of elasticity. A two-dimensional global higher-order deformation theory has been employed by Matsunaga (2009) for thermal buckling of FG plates. Zhao *et al*. (2009) presented the mechanical and thermal buckling analysis of FG ceramic–metal plates using the first-order shear deformation plate theory, in conjunction with the Ritz method. Also, Fuchiyama and Noda (1995) considered an FG plate made of ZrO_2 and Ti 6Al 4V under thermal loading. Zenkour (2009) presented a thermoelastic bending analysis of FG plates on elastic foundations. Using a trigonometric shear deformation plate theory, Zenkour and Alghamdi (2010) studied the bending response of sandwich FG plates subjected to thermomechanical loads. Zenkour and Sobhy (2010) investigated the thermal buckling of FG sandwich plates using trigonometric shear deformation plate theory.

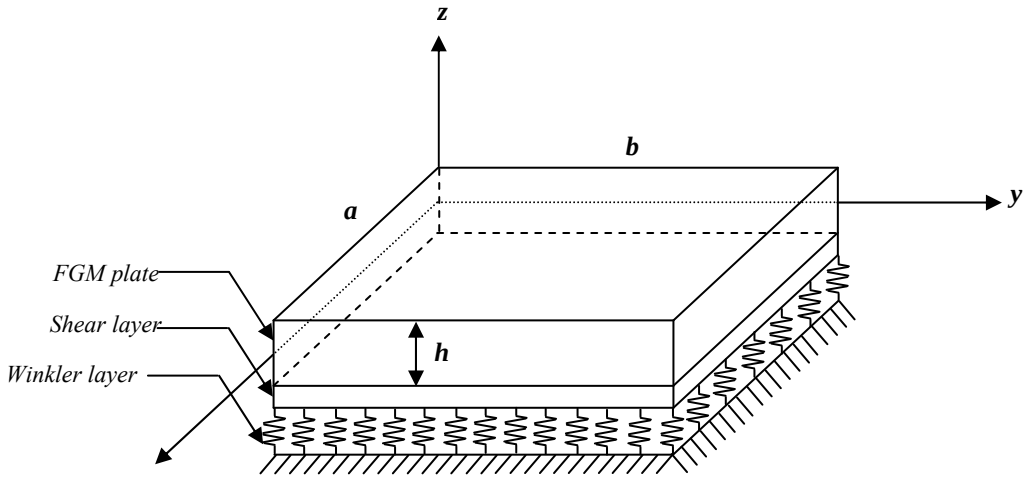

Fig. 1 Coordinate system and geometry for rectangular FG plates on Pasternak elastic foundation

In the present paper, an analytical solution to the thermomechanical bending response of FG plates resting on Winkler-Pasternak elastic foundations is developed using a refined trigonometric shear deformation theory (RTSDT) recently developed by Tounsi *et al.* (2012). Other shears deformation theories available in the literature (Reddy 2000, Zenkour and Alghamdi 2010, Zenkour and Sobhy 2010), are presented and studied for comparisons. The present refined trigonometric shear deformation theory is based on assumption that the in-plane and transverse displacements consist of bending and shear components in which the bending components do not contribute toward shear forces and, likewise, the shear components do not contribute toward bending moments. Unlike the conventional trigonometric shear deformation theory (Zenkour and Alghamdi 2010, Zenkour and Sobhy 2010), the proposed trigonometric shear deformation theory contains four unknowns. Material properties of FG plate are assumed to vary according to power law distribution of the volume fraction of the constituents. The results based on the present refined trigonometric shear deformation theory are compared with those obtained by the higher- and first-order shear deformation plate theories and classical plate theory. The influences of several parameters are discussed.

2. Theoretical formulation

Consider a functionally graded plate of thickness h, side length a in the x-direction, and b in the y-direction resting on Winkler-Pasternak elastic foundations as shown in Fig. 1. The refined trigonometric shear deformation plate theory used by Tounsi *et al.* (2012) accounts for trigonometric distribution of transverse shear stress, and satisfies the free transverse shear stress conditions on the top and bottom surfaces of the plate without using shear correction factor.

2.1 Basic assumptions

The assumptions of the present theory are as follows:

(1) The displacements are small in comparison with the plate thickness and, therefore, strains involved are infinitesimal.
(2) The transverse displacement w includes two components of bending w_b, and shear w_s. These components are functions of coordinates x, y only.

$$w(x, y, z) = w_b(x, y) + w_s(x, y) \tag{1}$$

(3) The transverse normal stress σ_z is negligible in comparison with in-plane stresses σ_x and σ_y.
(4) The displacements u in x-direction and v in y-direction consist of extension, bending, and shear components.

$$U = u_0 + u_b + u_s, \quad V = v_0 + v_b + v_s \tag{2}$$

The bending components u_b and v_b are assumed to be similar to the displacements given by the classical plate theory. Therefore, the expression for u_b and v_b can be given as

$$u_b = -z\frac{\partial w_b}{\partial x}, \quad v_b = -z\frac{\partial w_b}{\partial y} \tag{3}$$

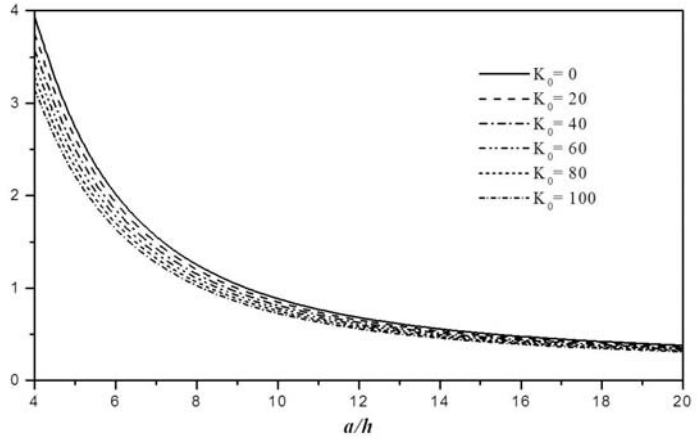

Fig. 2 Effect of Winkler modulus parameter on the dimensionless center deflection ($\overline{w}$) of a square FG plate ($k = 2$) for different side-to-thickness ratio a/h with $J_0 = 10$, $q_0 = 100$, $t_1 = 0$ and $t_2 = t_3 = 10$

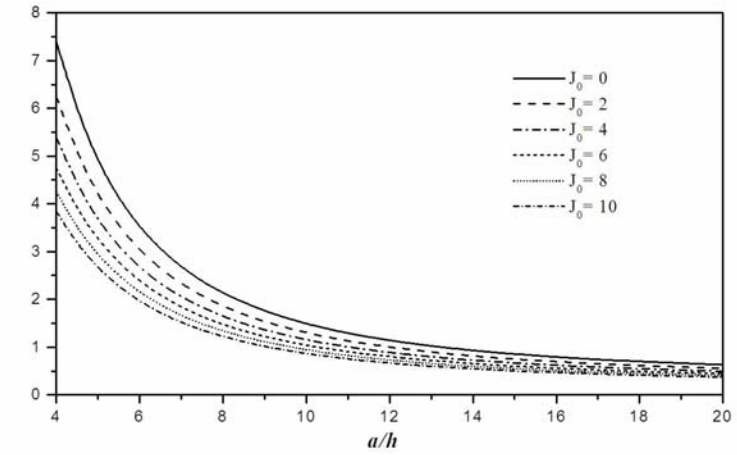

Fig. 3 Effect of Pasternak shear modulus parameter on the dimensionless center deflection ($\overline{w}$) of a square FG plate ($k = 2$) for different side-to-thickness ratio a/h with $k_0 = 10$, $q_0 = 100$, $t_1 = 0$ and $t_2 = t_3 = 10$.

The shear components u_s and v_s give rise, in conjunction with w_s, to the trigonometric variations of shear strains γ_{xz}, γ_{yz} and hence to shear stresses τ_{xz}, τ_{yz} through the thickness of the plate in such a way that shear stresses τ_{xz}, τ_{yz} are zero at the top and bottom faces of the plate. Consequently, the expression for u_s and v_s can be given as (Tounsi *et al.* 2012)

$$u_s = -f(z)\frac{\partial w_s}{\partial x}, \quad v_s = -f(z)\frac{\partial w_s}{\partial y} \tag{4}$$

where

$$f(z) = \left(z - \frac{h}{\pi}\sin\frac{\pi z}{h} \right) \tag{5}$$

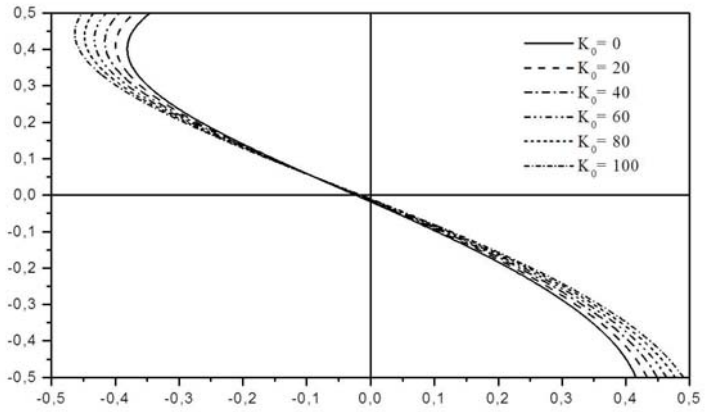

Fig. 4 Variation of dimensionless axial stress ($\bar{\sigma}_x$) through-the-thickness of a square FG plate (k = 2) for different values of Winkler modulus parameter k_0 with J_0 = 10, q_0 = 100, t_1 = 0 and t_2 = t_3 = 10 and a/h = 10

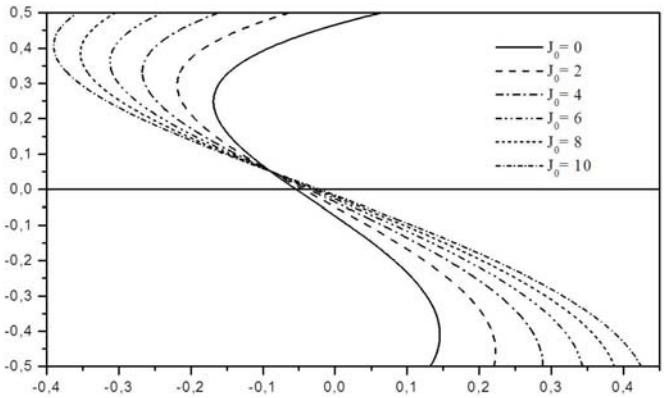

Fig. 5 Variation of dimensionless axial stress ($\bar{\sigma}_x$) through-the-thickness of a square FG plate (k = 2) for different values of Pasternak shear modulus parameter J_0 with k_0 = 10, q_0 = 100, t_1 = 0 and t_2 = t = 10 and a/h = 10

2.2. Kinematics

Based on the assumptions made in the preceding section, the displacement field can be obtained using Eqs. (1)-(5) as

$$\begin{aligned} u(x,y,z) &= u_0(x,y) - z\frac{\partial w_b}{\partial x} - f(z)\frac{\partial w_s}{\partial x} \\ v(x,y,z) &= v_0(x,y) - z\frac{\partial w_b}{\partial y} - f(z)\frac{\partial w_s}{\partial y} \\ w(x,y,z) &= w_b(x,y) + w_s(x,y) \end{aligned} \tag{6}$$

The kinematic relations can be obtained as follows

$$\begin{Bmatrix} \varepsilon_x \\ \varepsilon_y \\ \gamma_{xy} \end{Bmatrix} = \begin{Bmatrix} \varepsilon_x^0 \\ \varepsilon_y^0 \\ \gamma_{xy}^0 \end{Bmatrix} + z \begin{Bmatrix} k_x^b \\ k_y^b \\ k_{xy}^b \end{Bmatrix} + f(z) \begin{Bmatrix} k_x^s \\ k_y^s \\ k_{xy}^s \end{Bmatrix}, \quad \begin{Bmatrix} \gamma_{yz} \\ \gamma_{xz} \end{Bmatrix} = g(z) \begin{Bmatrix} \gamma_{yz}^s \\ \gamma_{xz}^s \end{Bmatrix} \tag{7}$$

where

$$\begin{Bmatrix} \varepsilon_x^0 \\ \varepsilon_y^0 \\ \gamma_{xy}^0 \end{Bmatrix} = \begin{Bmatrix} \dfrac{\partial u_0}{\partial x} \\ \dfrac{\partial v_0}{\partial x} \\ \dfrac{\partial u_0}{\partial y} + \dfrac{\partial v_0}{\partial x} \end{Bmatrix}, \quad \begin{Bmatrix} k_x^b \\ k_y^b \\ k_{xy}^b \end{Bmatrix} = \begin{Bmatrix} -\dfrac{\partial^2 w_b}{\partial x^2} \\ -\dfrac{\partial^2 w_b}{\partial y^2} \\ -2\dfrac{\partial^2 w_b}{\partial x \partial y} \end{Bmatrix}, \quad \begin{Bmatrix} k_x^s \\ k_y^s \\ k_{xy}^s \end{Bmatrix} = \begin{Bmatrix} -\dfrac{\partial^2 w_s}{\partial x^2} \\ -\dfrac{\partial^2 w_s}{\partial y^2} \\ -2\dfrac{\partial^2 w_s}{\partial x \partial y} \end{Bmatrix}, \quad \begin{Bmatrix} \gamma_{yz}^s \\ \gamma_{xz}^s \end{Bmatrix} = \begin{Bmatrix} \dfrac{\partial w_s}{\partial y} \\ \dfrac{\partial w_s}{\partial x} \end{Bmatrix} \tag{8a}$$

and

$$g(z) = 1 - \frac{df(z)}{dz} = \cos\left(\frac{\pi z}{h}\right) \tag{8b}$$

2.3. Constitutive equations

The plate is subjected to a sinusoidally distributed load $q(x,y)$ and a temperature field $T(x,y,z)$. The material properties P of the FG plate, such as Young's modulus E, Poisson's ratio v, and thermal expansion coefficient α are given according the formula

$$P(z) = P_M + (P_C - P_M)\left(\frac{1}{2} + \frac{z}{h}\right)^k \tag{9}$$

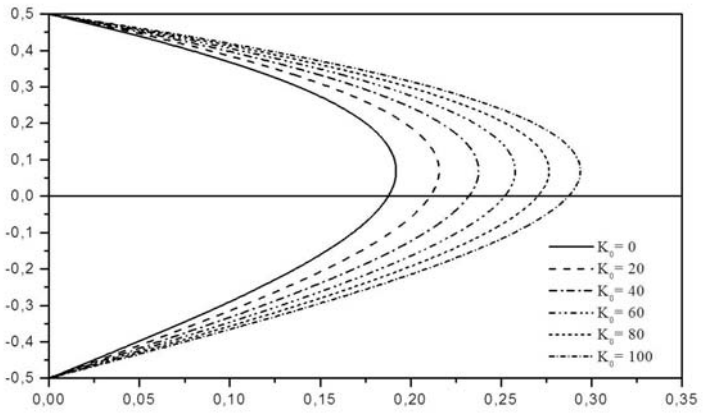

Fig. 6 Variation of dimensionless shear stress ($\bar{\tau}_{xz}$) through-the-thickness of a square FG plate (k = 2) for different values of Winkler modulus parameter k_0 with J_0 = 10, q_0 = 100, t_1 0 and $t_2 = t_3$ = 10 and a/h = 10

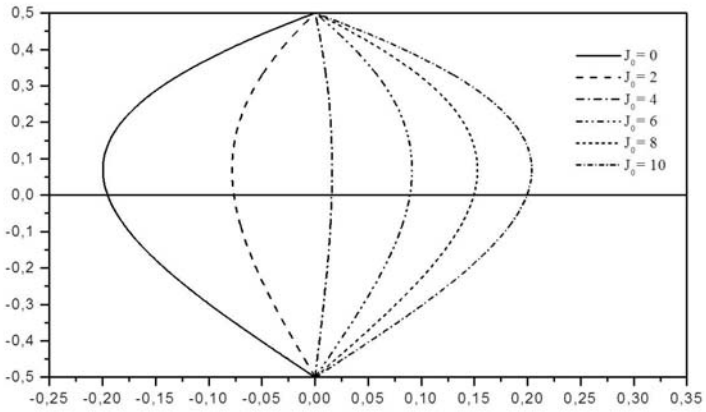

Fig. 7 Variation of dimensionless shear stress ($\bar{\tau}_{xz}$) through-the-thickness of a square FG plate (k = 2) for different values of Pasternak shear modulus parameter J_0 with k_0 = 10, q_0 = 100, t_1 = 0 and t_2 = t_3 = 10 and a/h = 10

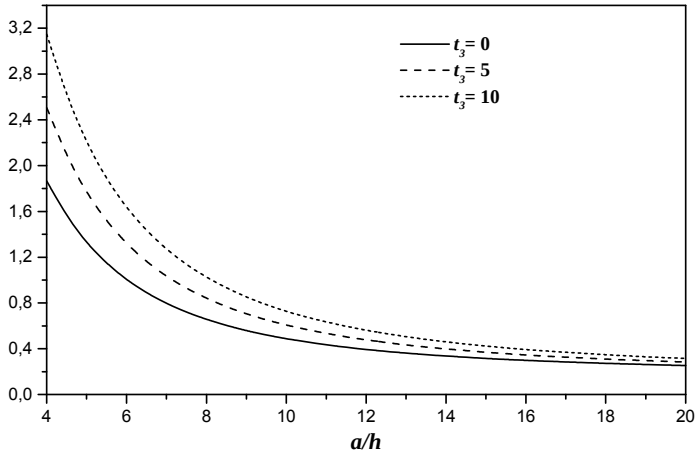

Fig. 8 Effect of the thermal load $t_3$on the dimensionless center deflection ($\bar{w}$) of a square FG plate (k = 2) for different side-to-thickness ratio a/h with k_0 = 100, J_0 = 10, q_0 = 100, t_1 = 0 and t_2 = 10

where P_C and P_M are the corresponding properties of the ceramic and metal, respectively, and k is the volume fraction exponent which takes values greater than or equal to zero.

The linear constitutive relations are

$$\begin{Bmatrix}\sigma_x\\ \sigma_y\\ \tau_{xy}\end{Bmatrix}=\begin{bmatrix}Q_{11} & Q_{12} & 0\\ Q_{12} & Q_{22} & 0\\ 0 & 0 & Q_{66}\end{bmatrix}\begin{Bmatrix}\varepsilon_x-\alpha\,\Delta T\\ \varepsilon_y-\alpha\,\Delta T\\ \gamma_{xy}\end{Bmatrix}\text{ and }\begin{Bmatrix}\tau_{yz}\\ \tau_{zx}\end{Bmatrix}=\begin{bmatrix}Q_{44} & 0\\ 0 & Q_{55}\end{bmatrix}\begin{Bmatrix}\gamma_{yz}\\ \gamma_{zx}\end{Bmatrix} \tag{10}$$

where (σ_x, σ_y, τ_{xy}, τ_{yz}, τ_{yx}) and (ε_x, ε_y, γ_{xy}, γ_{yz}, γ_{yx}) are the stress and strain components, respectively. Using the material properties defined in Eq. (9), stiffness coefficients, Q_{ij}, can be expressed as

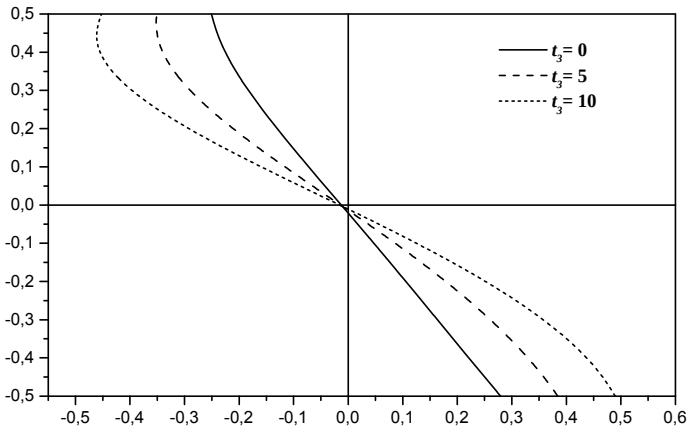

Fig. 9 Effect of the thermal load t_3 on the dimensionless axial stress ($\overline{\sigma}_x$) through-the-thickness of a square FG plate ($k = 2$) with $a/h = 10$, $k_0 = 100$, $J_0 = 10$, $q_0 = 100$, $t_1 = 0$ and $t_2 = 10$

$$Q_{11} = Q_{22} = \frac{E(z)}{1-\nu^2}, \tag{11a}$$

$$Q_{12} = \frac{\nu\, E(z)}{1-\nu^2}, \tag{11b}$$

$$Q_{44} = Q_{55} = Q_{66} = \frac{E(z)}{2(1+\nu)}, \tag{11c}$$

where $\Delta T = T - T_0$ in which T_0 is the reference temperature.

The applied temperature distribution $T(x,y,z)$ through the thickness are assumed, respectively, to be

$$T(x,y,z) = T_1(x,y) + \frac{z}{h}T_2(x,y) + \frac{1}{\pi}\sin\left(\frac{\pi z}{h}\right)T_3(x,y), \tag{12}$$

2.4. Governing equations

The governing equations of equilibrium can be derived by using the principle of virtual displacements. The principle of virtual work in the present case yields

$$\int_{-h/2}^{h/2}\int_{\Omega}\left[\sigma_x\delta\varepsilon_x + \sigma_y\delta\varepsilon_y + \tau_{xy}\delta\gamma_{xy} + \tau_{yz}\delta\gamma_{yz} + \tau_{xz}\delta\gamma_{xz}\right]d\Omega\, dz - \int_{\Omega}(q - f_e)\delta w d\Omega = 0 \tag{13}$$

where Ω is the top surface, and f_e is the density of reaction force of foundation. For the Pasternak foundation model

$$f_e = K_W w - J_1\frac{\partial^2 w}{\partial x^2} - J_2\frac{\partial^2 w}{\partial y^2} \tag{14}$$

where K_W is the modulus of subgrade reaction (elastic coefficient of the foundation) and J_1 and J_2 are the shear moduli of the subgrade (shear layer foundation stiffness). If foundation is homogeneous and isotropic, we will get $J_1 = J_2 = J_0$. If the shear layer foundation stiffness is neglected, Pasternak foundation becomes a Winkler foundation.

Substituting Eqs. (7) and (10) into Eq.(13) and integrating through the thickness of the plate, Eq. (13) can be rewritten as

$$\int_{\Omega}\left[N_x\delta\varepsilon_x^0 + N_y\delta\varepsilon_y^0 + N_{xy}\delta\varepsilon_{xy}^0 + M_x^b\delta k_x^b + M_y^b\delta k_y^b + M_{xy}^b\delta k_{xy}^b + M_x^s\delta k_x^s + M_y^s\delta k_y^s + M_{xy}^s\delta k_{xy}^s + S_{yz}^s\delta\gamma_{yz}^s + S_{xz}^s\delta\gamma_{xz}^s\right]d\Omega - \int_{\Omega}(q-f_e)(\delta w_b + \delta w_s)d\Omega = 0 \tag{15}$$

The stress resultants N, M, and S are defined by

$$\begin{Bmatrix} N_x, & N_y, & N_{xy} \\ M_x^b, & M_y^b, & M_{xy}^b \\ M_x^s, & M_y^s, & M_{xy}^s \end{Bmatrix} = \int_{-h/2}^{h/2}\left(\sigma_x, \sigma_y, \tau_{xy}\right)\begin{Bmatrix} 1 \\ z \\ f(z) \end{Bmatrix}dz, \tag{16a}$$

$$\left(S_{xz}^s, S_{yz}^s\right) = \int_{-h/2}^{h/2}\left(\tau_{xz}, \tau_{yz}\right)g(z)dz. \tag{16b}$$

Substituting Eq. (10) into Eq. (16) and integrating through the thickness of the plate, the stress resultants are given as

$$\begin{Bmatrix} N \\ M^b \\ M^s \end{Bmatrix} = \begin{bmatrix} A & B & B^s \\ B & D & D^s \\ B^s & D^s & H^s \end{bmatrix}\begin{Bmatrix} \varepsilon \\ k^b \\ k^s \end{Bmatrix} - \begin{Bmatrix} N^T \\ M^{bT} \\ M^{sT} \end{Bmatrix}, \quad S = A^s\gamma, \tag{17}$$

where

$$N = \left\{N_x, N_y, N_{xy}\right\}^t, \quad M^b = \left\{M_x^b, M_y^b, M_{xy}^b\right\}^t, \quad M^s = \left\{M_x^s, M_y^s, M_{xy}^s\right\}^t, \tag{18a}$$

$$N^T = \left\{N_x^T, N_y^T, 0\right\}^t, \quad M^{bT} = \left\{M_x^{bT}, M_y^{bT}, 0\right\}^t, \quad M^{sT} = \left\{M_x^{sT}, M_y^{sT}, 0\right\}^t, \tag{18b}$$

$$\varepsilon = \left\{\varepsilon_x^0, \varepsilon_y^0, \gamma_{xy}^0\right\}^t, \quad k^b = \left\{k_x^b, k_y^b, k_{xy}^b\right\}^t, \quad k^s = \left\{k_x^s, k_y^s, k_{xy}^s\right\}^t, \tag{18c}$$

$$A = \begin{bmatrix} A_{11} & A_{12} & 0 \\ A_{12} & A_{22} & 0 \\ 0 & 0 & A_{66} \end{bmatrix}, \quad B = \begin{bmatrix} B_{11} & B_{12} & 0 \\ B_{12} & B_{22} & 0 \\ 0 & 0 & B_{66} \end{bmatrix}, \quad D = \begin{bmatrix} D_{11} & D_{12} & 0 \\ D_{12} & D_{22} & 0 \\ 0 & 0 & D_{66} \end{bmatrix}, \tag{18d}$$

$$B^s = \begin{bmatrix} B_{11}^s & B_{12}^s & 0 \\ B_{12}^s & B_{22}^s & 0 \\ 0 & 0 & B_{66}^s \end{bmatrix}, \quad D^s = \begin{bmatrix} D_{11}^s & D_{12}^s & 0 \\ D_{12}^s & D_{22}^s & 0 \\ 0 & 0 & D_{66}^s \end{bmatrix}, \quad H^s = \begin{bmatrix} H_{11}^s & H_{12}^s & 0 \\ H_{12}^s & H_{22}^s & 0 \\ 0 & 0 & H_{66}^s \end{bmatrix}, \tag{18e}$$

$$S=\left\{S_{yz}^{s},S_{xz}^{s}\right\}^{t},\quad \gamma=\left\{\gamma_{yz},\gamma_{xz}\right\}^{t},\quad A^{s}=\begin{bmatrix}A_{44}^{s} & 0\\ 0 & A_{55}^{s}\end{bmatrix}, \tag{18f}$$

where A_{ij}, B_{ij}, etc., are the plate stiffness, defined by

$$\begin{Bmatrix}A_{11} & B_{11} & D_{11} & B_{11}^{s} & D_{11}^{s} & H_{11}^{s}\\ A_{12} & B_{12} & D_{12} & B_{12}^{s} & D_{12}^{s} & H_{12}^{s}\\ A_{66} & B_{66} & D_{66} & B_{66}^{s} & D_{66}^{s} & H_{66}^{s}\end{Bmatrix}=\int_{-h/2}^{h/2}Q_{11}\left(1,z,z^{2},f(z),z\,f(z),f^{2}(z)\right)\begin{Bmatrix}1\\ \nu\\ \dfrac{1-\nu}{2}\end{Bmatrix}dz, \tag{19a}$$

and

$$\left(A_{22},B_{22},D_{22},B_{22}^{s},D_{22}^{s},H_{22}^{s}\right)=\left(A_{11},B_{11},D_{11},B_{11}^{s},D_{11}^{s},H_{11}^{s}\right),\quad Q_{11}=\frac{E(z)}{1-\nu^{2}} \tag{19b}$$

$$A_{44}^{s}=A_{55}^{s}=\int_{-h/2}^{h/2}\frac{E(z)}{2(1+\nu)}\left[g(z)\right]^{2}dz, \tag{19c}$$

The stress and moment resultants, $N_x^T=N_y^T$, $M_x^{bT}=M_y^{bT}$, $M_x^{sT}=M_y^{sT}$ due to thermal loading are defined respectively by

$$\begin{Bmatrix}N_x^{T}\\ M_x^{bT}\\ M_x^{sT}\end{Bmatrix}=\int_{-h/2}^{h/2}\frac{E(z)}{1-\nu}\alpha(z)T\begin{Bmatrix}1\\ z\\ f(z)\end{Bmatrix}dz, \tag{20}$$

The governing equations of equilibrium can be derived from Eq. (15) by integrating the displacement gradients by parts and setting the coefficients δu_0, δv_0, δw_b and δw_s zero separately. Thus one can obtain the equilibrium equations associated with the present shear deformation theory

$$\begin{aligned}
&\delta u_0:\ \frac{\partial N_x}{\partial x}+\frac{\partial N_{xy}}{\partial y}=0\\
&\delta v_0:\ \frac{\partial N_{xy}}{\partial x}+\frac{\partial N_y}{\partial y}=0\\
&\delta w_b:\ \frac{\partial^2 M_x^b}{\partial x^2}+2\frac{\partial^2 M_{xy}^b}{\partial x\partial y}+\frac{\partial^2 M_y^b}{\partial y^2}-f_e+q=0\\
&\delta w_s:\ \frac{\partial^2 M_x^s}{\partial x^2}+2\frac{\partial^2 M_{xy}^s}{\partial x\partial y}+\frac{\partial^2 M_y^s}{\partial y^2}+\frac{\partial S_{xz}^s}{\partial x}+\frac{\partial S_{yz}^s}{\partial y}-f_e+q=0
\end{aligned} \tag{21}$$

Substituting from Eq. (17) into Eq. (21), we obtain the following equation

$$\begin{aligned}
&A_{11}d_{11}u_0+A_{66}d_{22}u_0+\left(A_{12}+A_{66}\right)d_{12}v_0-B_{11}d_{111}w_b-\left(B_{12}+2B_{66}\right)d_{122}w_b\\
&\quad-\left(B_{12}^{s}+2B_{66}^{s}\right)d_{122}w_s-B_{11}^{s}d_{111}w_s=p_1,
\end{aligned} \tag{22a}$$

$$A_{22}d_{22}v_0 + A_{66}d_{11}v_0 + (A_{12} + A_{66})d_{12}u_0 - B_{22}d_{222}w_b - (B_{12} + 2B_{66})d_{112}w_b - (B^s_{12} + 2B^s_{66})d_{112}w_s - B^s_{22}d_{222}w_s = p_2, \tag{22b}$$

$$B_{11}d_{111}u_0 + (B_{12} + 2B_{66})d_{122}u_0 + (B_{12} + 2B_{66})d_{112}v_0 + B_{22}d_{222}v_0 - D_{11}d_{1111}w_b - 2(D_{12} + 2D_{66})d_{1122}w_b - D_{22}d_{2222}w_b - D^s_{11}d_{1111}w_s - 2(D^s_{12} + 2D^s_{66})d_{1122}w_s - D^s_{22}d_{2222}w_s = p_3 \tag{22c}$$

$$B^s_{11}d_{111}u_0 + (B^s_{12} + 2B^s_{66})d_{122}u_0 + (B^s_{12} + 2B^s_{66})d_{112}v_0 + B^s_{22}d_{222}v_0 - D^s_{11}d_{1111}w_b - 2(D^s_{12} + 2D^s_{66})d_{1122}w_b - D^s_{22}d_{2222}w_b - H^s_{11}d_{1111}w_s - 2(H^s_{12} + 2H^s_{66})d_{1122}w_s - H^s_{22}d_{2222}w_s + A^s_{55}d_{11}w_s + A^s_{44}d_{22}w_s = p_4 \tag{22d}$$

where $\{p\} = \{p_1, p_2, p_3, p_4\}^t$ is a generalized force vector, d_{ij}, d_{ijl} and d_{ijlm} are the following differential operators

$$d_{ij} = \frac{\partial^2}{\partial x_i \partial x_j}, \quad d_{ijl} = \frac{\partial^3}{\partial x_i \partial x_j \partial x_l}, \quad d_{ijlm} = \frac{\partial^4}{\partial x_i \partial x_j \partial x_l \partial x_m}, \quad d_i = \frac{\partial}{\partial x_i}, \ (i, j, l, m = 1,2). \tag{23a}$$

The components of the generalized force vector $\{p\}$ are given by

$$p_1 = \frac{\partial N^T_x}{\partial x}, \quad p_2 = \frac{\partial N^T_y}{\partial y}, \quad p_3 = f_e + q - \frac{\partial^2 M^{bT}_x}{\partial x^2} - \frac{\partial^2 M^{bT}_y}{\partial y^2}, \tag{23b}$$

$$p_4 = f_e + q - \frac{\partial^2 M^{sT}_x}{\partial x^2} - \frac{\partial^2 M^{sT}_y}{\partial y^2} \tag{23c}$$

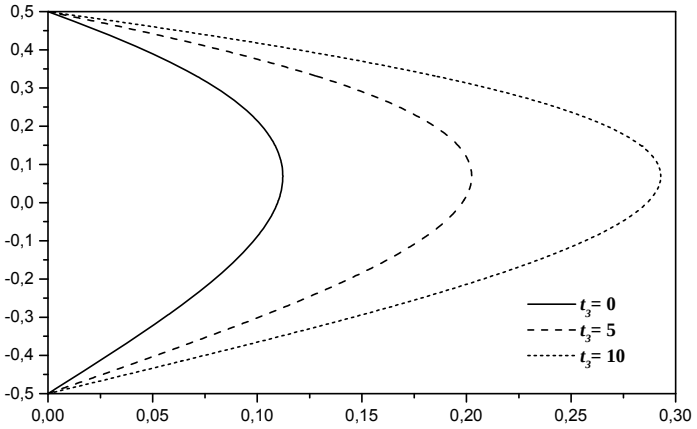

Fig. 10 Effect of the thermal load $t_3$on the dimensionless shear stress ($\bar{\tau}_{xz}$) through-the-thickness of a square FG plate ($k = 2$) with $a/h = 10$, $K_0 = 100$, $J_0 = 10$, $q_0 = 100$, $t_1 = 0$ and $t_2 = 10$

3. Exact solutions for FG plates

Rectangular plates are generally classified in accordance with the type of support used. We are here concerned with the exact solution of Eqs. (22) for a simply supported FG plate. To solve this problem, Navier assumed that the transverse mechanical and temperature loads, p and T_i in the form of a in the double Fourier series as

$$\begin{Bmatrix} q \\ T_i \end{Bmatrix} = \begin{Bmatrix} q_0 \\ t_i \end{Bmatrix} \sin(\lambda x)\sin(\mu y), \quad (i = 1, 2, 3) \tag{24}$$

where $\lambda = \pi / a$, $\mu = \pi / b$, q_0 and t_i are constants.

Following the Navier solution procedure, we assume the following solution form for u_0, v_0, w_b and w_s that satisfies the boundary conditions

$$\begin{Bmatrix} u_0 \\ v_0 \\ w_b \\ w_s \end{Bmatrix} = \begin{Bmatrix} U\cos(\lambda x)\sin(\mu y) \\ V\sin(\lambda x)\cos(\mu y) \\ W_b\sin(\lambda x)\sin(\mu y) \\ W_s\sin(\lambda x)\sin(\mu y) \end{Bmatrix}, \tag{25}$$

where U, V, W_b and W_s are arbitrary parameters to be determined subjected to the condition that the solution in Eq. (25) satisfies governing Eqs. (22). One obtains the following operator equation

$$[K]\{\Delta\} = \{P\}, \tag{26}$$

Where $\{\Delta\} = \{U, V, W_b, W_s\}^t$ and $[K]$ is the symmetric matrix given by

$$[K] = \begin{bmatrix} k_{11} & k_{12} & k_{13} & k_{14} \\ k_{12} & k_{22} & k_{23} & k_{24} \\ k_{13} & k_{23} & k_{33} & k_{34} \\ k_{14} & k_{24} & k_{34} & k_{44} \end{bmatrix}, \tag{27}$$

in which

$$\begin{aligned}
k_{11} &= -\left(A_{11}\lambda^2 + A_{66}\mu^2\right) \\
k_{12} &= -\lambda\,\mu\left(A_{12} + A_{66}\right) \\
k_{13} &= \lambda\left[B_{11}\lambda^2 + (B_{12} + 2B_{66})\,\mu^2\right] \\
k_{14} &= \lambda\left[B^s_{11}\lambda^2 + (B^s_{12} + 2B^s_{66})\,\mu^2\right] \\
k_{22} &= -\left(A_{66}\lambda^2 + A_{22}\mu^2\right) \\
k_{23} &= \mu\left[(B_{12} + 2B_{66})\,\lambda^2 + B_{22}\mu^2\right] \\
k_{24} &= \mu\left[(B^s_{12} + 2B^s_{66})\,\lambda^2 + B^s_{22}\mu^2\right] \\
k_{33} &= -\left(D_{11}\lambda^4 + 2(D_{12} + 2D_{66})\lambda^2\mu^2 + D_{22}\mu^4 + K_W + J_1\lambda^2 + J_2\mu^2\right) \\
k_{34} &= -\left(D^s_{11}\lambda^4 + 2(D^s_{12} + 2D^s_{66})\lambda^2\,\mu^2 + D^s_{22}\,\mu^4 + K_W + J_1\lambda^2 + J_2\mu^2\right) \\
k_{44} &= -\left(H^s_{11}\lambda^4 + 2(H^s_{11} + 2H^s_{66})\lambda^2\mu^2 + H^s_{22}\mu^4 + A^s_{55}\lambda^2 + A^s_{44}\mu^2 + K_W + J_1\lambda^2 + J_2\mu^2\right)
\end{aligned} \tag{28}$$

The components of the generalized force vector $\{P\} = \{P_1, P_2, P_3, P_4\}^t$ are given by

$$\begin{aligned} P_1 &= \lambda\left(A^T t_1 + B^T t_2 + {}^aB^T t_3\right), \\ P_2 &= \mu\left(A^T t_1 + B^T t_2 + {}^aB^T t_3\right), \\ P_3 &= -q_0 - h\left(\lambda^2 + \mu^2\right)\left(B^T t_1 + D^T t_2 + {}^aD^T t_3\right), \\ P_4 &= -q_0 - h\left(\lambda^2 + \mu^2\right)\left({}^sB^T t_1 + {}^sD^T t_2 + {}^sF^T t_3\right). \end{aligned} \tag{29}$$

where

$$\left\{A^T, B^T, D^T\right\} = \int_{-h/2}^{h/2} \frac{E(z)}{1-\nu}\alpha(z)\left\{1, \bar{z}, \bar{z}^2\right\}dz, \tag{30a}$$

$$\left\{{}^aB^T, {}^aD^T\right\} = \int_{-h/2}^{h/2} \frac{E(z)}{1-\nu}\alpha(z)\overline{\Psi}(z)\left\{1, \bar{z}\right\}dz, \tag{30b}$$

$$\left\{{}^sB^T, {}^sD^T, {}^sF^T\right\} = \int_{-h/2}^{h/2} \frac{E(z)}{1-\nu}\alpha(z)\overline{f}(z)\left\{1, \bar{z}, \overline{\Psi}(z)\right\}dz, \tag{30c}$$

in which $\bar{z} = z/h$, $\bar{f}(z) = f(z)/h$ and $\overline{\Psi}(z) = \frac{1}{\pi}\sin\left(\frac{\pi z}{h}\right)$.

4. Results and discussion

In this section, numerical examples are presented and discussed for verifying the accuracy of the present theory in predicting the thermomechanical bending responses of plates. Comparisons are made with various plate theories available in the literature. The description of various displacement models is given in Table 1.

The FGM plate is taken to be made of Titanium and Zirconia with the following material properties:

- Metal (Titanium, Ti-6Al-4V): E_M = 66.2 GPa; ν = 1/3; α_M = 10.3 × (10^{-6}/C°).
- Ceramic (Zirconia, ZrO_2): E_C = 117.0 GPa; ν = 1/3; α_C = 7.11 × (10^{-6}/C°).

The reference temperature is taken by T_0 = 25°C (room temperature). Numerical results are presented in terms of non-dimensional stresses and deflection. The various nondimensional parameters used are

Table 1 Displacement models

Model	Theory	Unknown functions
CPT	Classical plate theory	3
FSDT	First-order shear deformation theory (Whitney and Pagano, 1970)	5
PSDT	Parabolic shear deformation theory (Reddy, 2000)	5
TSDT	Trigonometric shear deformation theory (Zenkour, 2009)	5
Present	Present refined trigonometric shear deformation theory	4

- center deflection $\bar{w} = \frac{10^2 D}{a^4 q_0} w\left(\frac{a}{2}, \frac{b}{2}\right)$,
- axial stress $\bar{\sigma}_x = \frac{1}{10^2 q_0} \sigma_x\left(\frac{a}{2}, \frac{b}{2}, \frac{h}{2}\right)$,
- longitudinal shear stress $\bar{\tau}_{xy} = \frac{1}{10 q_0} \tau_{xy}\left(0,0,\frac{-h}{3}\right)$
- transversal shear stress $\bar{\tau}_{xz} = -\frac{1}{10 q_0} \tau_{xz}\left(0,\frac{b}{2},0\right)$,
- thickness coordinate $\bar{z} = z/h$.
- $K_0 = \frac{a^4 K_W}{D}$; $J_0 = \frac{a^2 J_1}{D} = \frac{b^2 J_2}{D}$, $D = \frac{h^3 E_C}{12\left(1-\nu^2\right)}$

Numerical results are tabulated in Tables 2-5 and plotted in Figs. 1-11 using the present refined trigonometric shear deformation theory (RTSDT). We note that the shear correction factor is taken K = 5/6 in FSDT.

The correlation between the present refined trigonometric shear deformation theory (RTSDT) and different higher-order and first-order shear deformation theories and classical plate theory is illustrated in Tables 2-4. These Tables give also the effects of the volume fraction exponent ratio *k* and elastic foundation parameters on the dimensionless deflection and stresses of FG rectangular plate.

Table 2 gives the effects of the volume fraction exponent ratio *k* and elastic foundation parameters on the dimensionless displacements and stresses of FG rectangular plate subjected to a mechanical load. It can be shown that the deflection and stresses are decreasing with the existence of the elastic foundations. The inclusion of the Winkler foundation parameter gives results more than those with the inclusion of Pasternak foundation parameters. As the volume fraction exponent increases for FG plates, the deflection will increase. The stresses are also sensitive to the variation of *k*.

Tables 3 and 4 present similar results as those given in Table 2 including the effect of the temperature field. The obtained results are compared with those predicted by FSDT, TSDT and PSDT. An excellent agreement is obtained between the present theory and the conventional TSDT (Zenkour 2009) for all values of power law index *k* and with or without the presence of the elastic foundation. It is important to observe that the stresses for a fully ceramic plate are not the same as that for a fully metal plate with elastic foundations. This is because the plate here is affected with the inclusion of the temperature field.

From results presented in Tables 2-4, it should be noted that the unknown function in present theory is four, while the unknown function in FSDT, PSDT and TSDT is five. It can be concluded that the present theory is not only accurate but also simple in predicting the thermomechanical bending response of FG plates resting on Winkler's or Pasternak's elastic foundations.

Table 5 gives the effects of side-to-thickness ratio and elastic foundation parameters on the dimensionless deflection of FG square plate under thermomechanical loads using the present refined trigonometric shear deformation theory (RTSDT). It is clear that the deflection decreases as the side-to-thickness ratio a/h increases. In addition, all displacements are decreasing with the existence of the elastic foundations. The inclusion of the Winkler foundation parameter gives results more than those with the inclusion of Pasternak foundation parameters.

Table 2 Effect of the volume fraction exponent and elastic foundation parameters on the dimensionless and stresses of an FG rectangular plate ($a = 10h$, $b = 2a$, $q_0 = 100$, $T = 0$).

K	K_0	J_0	Theory	$\overline{w}$	$\overline{\sigma}_x$	$\overline{\tau}_{xy}$	$\overline{\tau}_{xz}$
Ceramic	0	0	Present	0.68131	0.42424	0.86240	*-0.39400*
			PSDT	0.68134	0.42408	0.86253	*-0.38180*
			TSDT	0.68131	0.42424	0.86240	*-0.39400*
			FSDT	0.68135	0.42148	0.86459	*-0.30558*
			CPT	0.65704	0.42148	0.86459	–
	100	0	Present	0.40523	0.25233	0.51296	*-0.23435*
			PSDT	0.40524	0.25222	0.51300	*-0.22708*
			TSDT	0.40523	0.25233	0.51296	*-0.23435*
			FSDT	0.40525	0.25070	0.51426	*-0.18175*
			CPT	0.39652	0.25437	0.52183	–
	0	100	Present	0.083654	0.052093	0.10589	*-0.048377*
			PSDT	0.083655	0.052070	0.10590	*-0.046876*
			TSDT	0.083654	0.052093	0.10589	*-0.048377*
			FSDT	0.083655	0.051750	0.10615	*-0.037518*
			CPT	0.08328	0.05342	0.10959	–
	100	100	Present	0.077197	0.048071	0.097724	*-0.044643*
			PSDT	0.077197	0.048050	0.097731	*-0.043259*
			TSDT	0.077197	0.048071	0.097724	*-0.044643*
			FSDT	0.077198	0.047754	0.097959	*-0.034622*
			CPT	0.07688	0.04932	0.10116	–
0.5	100	100	Present	0.078729	0.045788	0.081728	*-0.038066*
			PSDT	0.078730	0.045766	0.081731	*-0.036901*
			TSDT	0.078729	0.045788	0.081728	*-0.038066*
			FSDT	0.078732	0.045460	0.081870	*-0.029835*
			CPT	0.078463	0.04693	0.08451	–
1	100	100	Present	0.079321	0.044892	0.073054	*-0.035023*
			PSDT	0.079322	0.044871	0.073061	*-0.033939*
			TSDT	0.079321	0.044892	0.073054	*-0.035023*
			FSDT	0.079322	0.044575	0.073208	*-0.027163*
			CPT	0.07907	0.04604	0.07561	–
2	100	100	Present	0.079758	0.044595	0.067185	*-0.032215*
			PSDT	0.079758	0.044574	0.067192	*-0.031170*
			TSDT	0.079758	0.044595	0.067185	*-0.032215*
			FSDT	0.079753	0.044297	0.067395	*-0.024345*
			CPT	0.07950	0.04581	0.06969	–
5	100	100	Present	0.080150	0.045736	0.064125	*-0.029922*
			PSDT	0.080150	0.045714	0.064136	*-0.028921*
			TSDT	0.080150	0.045736	0.064125	*-0.029922*
			FSDT	0.080141	0.045462	0.064399	*-0.022053*
			CPT	0.07989	0.04710	0.06672	–
Metal	100	100	Present	0.081190	0.050559	0.058148	*-0.026565*
			PSDT	0.081191	0.050538	0.058155	*-0.025744*
			TSDT	0.081190	0.050559	0.058148	*-0.026565*
			FSDT	0.081191	0.050227	0.058294	*-0.020603*
			CPT	*0.08099*	*0.05196*	*0.06030*	–

Table 3 Effect of the volume fraction exponent and elastic foundation parameters on the dimensionless and stresses of an FG rectangular plate ($a/h = 10$, $b = 2a$, $q_0 = 100$, $\overline{T}_1 = \overline{T}_3 = 0$, $\overline{T}_2 = 10$)

k	K_0	J_0	Theory	$\overline{w}$	$\overline{\sigma}_x$	$\overline{\tau}_{xy}$	$\overline{\tau}_{xz}$
Ceramic	0	0	Present	1.5241	0.34104	1.97150	-0.39400
			PSDT	1.5243	0.34091	1.97170	-0.38180
			TSDT	1.5241	0.34104	1.97150	-0.39400
			FSDT	1.5242	0.33831	1.97387	-0.30558
	100	0	Present	0.90655	-0.04355	1.18980	-0.03682
			PSDT	0.90655	-0.04356	1.18980	-0.03568
			TSDT	0.90655	-0.04355	1.18980	-0.03682
			FSDT	0.90654	-0.04379	1.18990	-0.02856
	0	100	Present	0.18714	-0.49153	0.27911	0.37921
			PSDT	0.18714	-0.49134	0.27905	0.36745
			TSDT	0.18714	-0.49153	0.27911	0.37921
			FSDT	0.18714	-0.48884	0.27706	0.29409
	100	100	Present	0.17270	-0.50052	0.26082	0.38756
			PSDT	0.17270	-0.50034	0.26075	0.37555
			TSDT	0.17270	-0.50052	0.26082	0.38756
			FSDT	0.17270	-0.49778	0.25873	-0.30057
0.5	100	100	Present	0. 17184	-0.49679	0.19609	0.38693
			PSDT	0.17183	-0.49659	0.19089	0.37511
			TSDT	0. 17184	-0.49679	0.19609	0.38693
			FSDT	0. 17180	-0.49350	0.18949	0.30356
1	100	100	Present	0.16978	-0.49047	0.15150	0.37510
			PSDT	0.16978	-0.49024	0.15145	0.36342
			TSDT	0.16978	-0.49047	0.15150	0.37510
			FSDT	0.16977	-0.48711	0.14980	0.29033
2	100	100	Present	0.16819	-0.48398	0.12850	0.35985
			PSDT	0.16819	-0.48375	0.12840	0.34801
			TSDT	0.16819	-0.48398	0.12850	0.35985
			FSDT	0.16825	0.48075	0.12602	0.27047
5	100	100	Present	0.16719	-0.48223	0.12836	0.34986
			PSDT	0.16720	-0.48201	0.12822	0.33789
			TSDT	0.16719	-0.48223	0.12836	0.34986
			FSDT	0.16733	-0.47920	0.12497	0.25580
Metal	100	100	Present	0.16353	-0.49911	0.15172	0.34603
			PSDT	0.16351	-0.49881	0.15166	0.33531
			TSDT	0.16353	-0.49911	0.15172	0.34603
			FSDT	0.16351	-0.49478	0.14985	0.26836

The effect of foundation stiffness and side-to-thickness ratio on the dimensionless deflection of FG square FG plate ($k = 2$) is shown in Figs. 2 and 3. It can be seen that the increase of side-to-thickness ratio a/h leads to a decrease of the center deflection of the FG plate. Furthermore, it is seen from Fig. 2 that as the Winkler modulus parameter increase the center deflection of the FG plate decreases. This decreasing trend is attributed to the stiffness of the elastic medium. In addition, it can be observed from Fig. 3 that as the shear modulus parameter increases, the center

Table 4 Effect of the volume fraction exponent and elastic foundation parameters on the dimensionless and stresses of an FG rectangular plate ($a/h = 10$, $b = 2a$, $q_0 = 100$, $\overline{T}_1 = 10$, $\overline{T}_2 = \overline{T}_3 = 0$)

k	K_0	J_0	Theory	$\overline{w}$	$\overline{\sigma}_x$	$\overline{\tau}_{xy}$	$\overline{\tau}_{xz}$
Ceramic	0	0	Present	2.1762	0.36232	2.8301	*-0.38826*
			PSDT	2.1982	0.35746	2.8590	*-0.37714*
			TSDT	2.1762	0.36232	2.8301	*-0.38826*
	100	0	Present	1.2943	-0.18687	1.7137	*0.12172*
			PSDT	1.3074	-0.19699	1.7314	*0.12203*
			TSDT	1.2943	-0.18687	1.7137	*0.12172*
	0	100	Present	0.26722	-0.82640	0.41361	*0.71573*
			PSDT	0.26989	-0.84276	0.41791	*0.70345*
			TSDT	0.26722	-0.82640	0.41361	*0.71573*
	100	100	Present	0.24658	-0.83925	0.38749	*0.72767*
			PSDT	0.24906	-0.85572	0.39153	*0.71512*
			TSDT	0.24658	-0.83925	0.38749	*0.72767*
0.5	100	100	Present	0.24403	-0.83097	0.27656	*0.72198*
			PSDT	0.24643	-0.84723	0.27923	*0.70975*
			TSDT	0.24403	-0.83097	0.27656	*0.72198*
1	100	100	Present	0.23987	-0.81888	0.21276	*0.69830*
			PSDT	0.24222	-0.83494	0.21462	*0.68600*
			TSDT	0.23987	-0.81888	0.21276	*0.69830*
2	100	100	Present	0.23656	-0.80694	0.17576	*0.66812*
			PSDT	0.23886	-0.82284	0.17714	*0.65525*
			TSDT	0.23656	-0.80694	0.17576	*0.66812*
5	100	100	Present	0.23434	-0.80533	0.17862	*0.64769*
			PSDT	0.23662	-0.82118	0.17992	*0.63442*
			TSDT	0.23434	-0.80533	0.17862	*0.64769*
Metal	100	100	Present	0.22721	-0.83863	0.22451	*0.63900*
			PSDT	0.22935	-0.85494	0.22677	*0.62785*
			TSDT	*0.22721*	*-0.83863*	*0.22451*	*0.63900*

deflection of the FG plate decreases considerably for thick FG plate. However, for thin plates, the effect of foundation stiffness tends to become less.

The axial stress, $\overline{\sigma}_x$, are plotted in Figs. 4 and 5. It can be seen that the maximum compressive stresses occur at a point near the top surface and the maximum tensile stresses occur, of course, at a point near the bottom surface of the FG plate. In addition, it can be observed from these figures that the elastic foundation has a significant effect on the maximum values of the axial stress, $\overline{\sigma}_x$.

It is observed that normal stress increases gradually with K_0 or J_0. However, the effect of Pasternak shears modulus parameter is more significant than Winkler modulus parameter.

Figs. 6 and 7 depict the through-the-thickness distributions of the shear stress $\overline{\tau}_{xz}$ in the FG square plates under the thermal loads (q_0 = 100, t_1 = 0 and $t_2 = t_3$ = 10). The volume fraction exponent of the FG plate is taken as k = 2. The through-the-thickness distributions of the shear stress $\overline{\tau}_{xz}$ are not parabolic in the FG plate and the stresses increase with increasing the foundation

Table 5 Effects of side-to-thickness ratio and elastic foundation parameters on the dimensionless deflection of an FG square plate ($q_0 = 100$, $\overline{T}_1 = 0$, $\overline{T}_2 = \overline{T}_3 = 10$)

k	K_0	J_0	a/h			
			5	10	20	*50*
Ceramic	0	0	4.0497	1.2060	0.49406	*0.29463*
	100	0	3.0746	0.94827	0.39198	*0.23435*
	0	100	0.55779	0.18947	0.080457	*0.048477*
	100	100	0.53445	0.18171	0.077180	*0.046508*
1	0	0	4.9217	1.4844	0.62354	*0.38238*
	100	0	3.4814	1.0949	0.46489	*0.28596*
	0	100	0.53692	0.18501	0.080594	*0.049942*
	100	100	0.51374	0.17716	0.077187	*0.047836*
2	0	0	5.1072	1.5476	0.65537	*0.40539*
	100	0	3.5349	1.1218	0.48075	*0.29837*
	0	100	0.52225	0.18223	0.080217	*0.050177*
	100	100	0.49953	0.17443	0.076803	*0.048043*
3	0	0	5.2006	1.5784	0.67020	*0.41571*
	100	0	3.5618	1.1352	0.48812	*0.30384*
	0	100	0.51578	0.18125	0.080135	*0.050284*
	100	100	0.49326	0.17347	0.076714	*0.048141*
4	0	0	5.2669	1.6000	0.68046	*0.42274*
	100	0	3.5823	1.1446	0.49319	*0.30755*
	0	100	0.51221	0.18073	0.080101	*0.050358*
	100	100	0.48980	0.17295	0.076673	*0.048208*
5	0	0	5.3201	1.6175	0.68878	*0.42850*
	100	0	3.5999	1.1523	0.49726	*0.31053*
	0	100	0.50995	0.18033	0.080067	*0.050416*
	100	100	0.48761	0.17256	0.076639	*0.048259*
Metal	0	0	5.9677	1.8338	0.79875	*0.50883*
	100	0	3.8241	1.2387	0.54697	*0.34979*
	0	100	0.49466	0.17493	0.079196	*0.051011*
	100	*100*	*0.47271*	*0.16727*	*0.075734*	*0.048787*

stress $\overline{\tau}_{xz}$ are not parabolic in the FG plate and the stresses increase with increasing the foundation parameters K_0 or J_0. The maximum values of $\overline{\tau}_{xz}$ occur at $\overline{z} \cong 0.1$ of the FG plate, not at the plate center as in the homogeneous case.

Finally, Figs. 8-10 show the effect of the thermal field t_3 on the deflection and stresses. The elastic foundation parameters are $K_0 = 100$ and $J_0 = 10$. The deflection and both axial stresses and shear stresses increase with the increase of the thermal load t_3.

5. Conclusions

A refined trigonometric shear deformation plate theory is used to study the thermomechanical bending behavior of functionally graded plates resting on Winkler-Pasternak elastic foundations. The theory contains only four unknown displacements and satisfies the zero traction boundary conditions at the plate's surfaces. The results of the shear deformation theories are compared together. The gradients in material properties play an important role in determining the response of the FG plates. However, the inclusion of the foundation parameters may give displacements and stresses with higher magnitudes. The mixture of the ceramic and metal with continuously varying volume fraction can eliminate interface problems of sandwich plates and thus the stresses distributions are smooth. All comparison studies demonstrated that the deflections and stresses obtained using the present refined theory (with four unknowns) and other higher-order shear deformation theories (five unknowns) are almost identical. In addition, unlike any other theory, the theory presented gives rise to only four governing equations resulting in considerably lower computational effort when compared with the other higher-order theories reported in the literature having more number of governing equations. Hence, it can be said that the proposed theory is accurate and simple in solving the thermomechanical bending behavior of FG plates resting on elastic foundations.

This theory can be implemented via a displacement based finite element method as is shown by Vo and Thai (2012). For this, the variational statement in Eq. (15) requires that the bending and shear components of transverse displacement w_b and w_s be twice differentiable and C^1-continuous, whereas the axial displacements u_0 and v_0 must be only once differentiable and C^0-continuous. Thus, a finite element formulation of the present theory will be considered in the future work to solve more complex problems.

References

Behravan Rad, A. (2012),"Static response of 2-D functionally graded circular plate with gradient thickness and elastic foundations to compound loads", *Struct. Eng. Mech.*, **44**(2).

Cheng, Z.Q. and Batra, R.C. (2000), "Three-dimensional thermoelastic deformations of a functionally graded elliptic plate", *Composites*, *Part B*, **31**(2), 97-106.

Filipich, C.P. and Rosales, M.B. (2002), "A further study about the behavior of foundation piles and beams in a Winkler-Pasternak soil", *Int. J. Mech. Sci.*, **44**(1), 21-36.

Fuchiyama, T. and Noda, N. (1995), "Analysis of thermal stress in a plate of functionally gradient material", *JSAE Rev*, **16**(3), 263-268.

Kerr, A.D. (1964), "Elastic and viscoelastic foundation models", *ASME J. Appl. Mech.*, **31**(3), 491-498.

Matsunaga, H. (2000), "Vibration and stability of thick plates on elastic foundations", *ASCE J. Eng. Mech.*, **126**(1), 27-34.

Matsunaga, H. (2009), "Thermal buckling of functionally graded plates according to a 2 D higher-order deformation theory", *Compos Struct*, **90**(1), 76-86.

Omurtag, M.H., Ozutok, A. and Akoz, A.Y. (1997), "Free vibration analysis of Kirchhoff plates resting on elastic foundation by mixed finite element formulation based on Gateaux differential", *Int. J. Numer. Methods. Eng.*, **40**(2), 295-317.

Pasternak, P.L. (1954), "On a new method of analysis of an elastic foundation by means of two foundation constants", *Cosudarstrennoe Izdatelstvo Literaturi po Stroitelstvu i Arkhitekture*, Moscow, 1-56 [In Russian].

Reddy, J.N. (2000), "Analysis of Functionally Graded Plates", *Int. J. Numer. Methods Eng.*, **47**, 663-684.

Reddy, J.N. and Cheng, Z.Q. (2001), "Three-dimensional thermomechanical deformations of functionally graded rectangular plates", *European J. of Mech*., *A*/*Solids*, **20**(5), 841-855.
Tounsi, A., Houari, M.S.A., Benyoucef, S. and Adda Bedia, E.A. (2012), "A refined trigonometric shear deformation theory for thermoelastic bending of functionally graded sandwich plates", *Aerospace Sci*. *and Technol*., (In press).
Vel, S.S., Batra, R.C. (2002), "Exact Solution for Thermoelastic Deformations of Functionally Graded Thick Rectangular Plates", *AIAA J*., **40**(7), 1421-1433.
Vo, T.P. and Thai, H.T. (2012), "Vibration and buckling of composite beams using refined shear deformation theory", *Inter*. *J*. *Mech*. *Sci*., **62**, 67-76.
Whitney, J.M. and Pagano. N.J. (1970), "Shear deformation in heterogeneous anisotropic plates", *J*. *Appl*. *Mech*., **37**, 1031-1036.
Ying, J., Lü, C.F. and Lim, C.W. (2009), "3D thermoelasticity solutions for functionally graded thick plates", *J*. *Zhejiang Univ*. *Sci*. *A*, **10**(3), 327-336.
Zenkour, A.M. (2009), "The refined sinusoidal theory for FGM plates on elastic foundations", *Inter*. *J*. *of* Mech. *Sci*., **51**(11-12), 869-880.
Zenkour, A.M. and Alghamdi, N.A. (2010), "Bending analysis of functionally graded sandwich plates under the effect of mechanical and thermal loads", *Mech*. *of Advanced Mater*. *and Struct*., **17**(6), 419-432.
Zenkour, A.M. and Sobhy, M. (2010), "Thermal buckling of various types of FGM sandwich plates", *Compos*. *Struct*., **93**(1), 93-102.
Zhao, X., Lee, Y.Y. and Liew, KM. (2009), "Mechanical and thermal buckling analysis of functionally graded plates", *Compos*. *Struct*, **90**(2), 161-171.
Zhou, D., Cheung, Y.K., Lo, S.H. and Au, F.T.K. (2004), "Three-dimensional vibration analysis of rectangular thick plates on Pasternak foundations", *Int*. *J*. *Numer*. *Methods Eng*., **59**(10), 1313-1334.

CC